Biomechanics of the Female Pelvic Floor
2016, Pages 259-277

Chapter Twelve - Dynamic Visualization of the Female Pelvic Floor Function

C.E. Constantinou

https://doi.org/10.1016/B978-0-12-803228-2.00012-X
Get rights and content

Abstract

The female pelvic floor (PF) is made up of a network of muscles and associated supporting structures organized to contain abdominal structures and their contents. This network is wired in such a way as to maintain the contents within it most of the time and expel only during voluntary commands. For many reasons, primarily age and parity, such a function is compromised, whereupon incontinence may occur. In this chapter, the mechanisms recruited to prevent incontinence are considered from a dynamic point of view in terms of their biomechanical actions by visualizing timing/displacement/force parameters. Ultrasound image analysis was used to parameterize the temporal sequence of displacement and a vaginal probe force distribution. Stimuli to simulate conditions of incontinence were the cough reflex, a common triggering mechanism generating incontinence. Voluntary activation of the PF by contraction was evaluated to estimate the strength of the contraction generated. Collectively, biomechanical metrics of the spatial/temporal distribution of these stimuli were generated to indicate the differences between the continent and incontinent subjects. Among the metrics used are the trajectory of the landmarks displaced by each stimulus by segmenting and tracking the outlines of the bladder, urethra, and bowel. From such measurements, the velocity and acceleration of the urethral opening were calculated as critical biomechanical parameters. From the segmented visualizations the strain generated by stress stimuli was computed and is considered. While parameterization of the dynamics of the various components of PF activity

provide important values underlying the mechanisms of continence, it is not yet practical with current technology to apply to clinical practice.

Previous Next

Keywords

Continence; Urethra; Bladder; Urinary reflexes; Ultrasound imaging; Biomechanics; Strain; Trajectory ; Segmentation

Acknowledgments

The support of NIH/NIBIB grants 1 R21 EB001654 and 1 R01 EB006170 is gratefully acknowledged.

Introduction

Previous chapters have shown that the pelvic cavity contains several organs that help to fulfill diverse roles, including sexual intercourse, conception, parturition, and solid and liquid storage and evacuation. These multiple organ systems interact and coordinate with each other in performing their normal physiological functions. Under certain conditions, some of these functions are subject to disruption, manifesting in pathologies such as incontinence and prolapse in a large percentage of women as well as any one of a spectrum of complex problems such as pain whose origin may or may not be readily identifiable. In this context, pelvic floor (PF) dysfunction constitutes a global burden affecting the quality of life of the individual, their family, and society in general. In women, because of the magnitude of the problem, a great deal of attention has been placed on the implication of the PF function as it relates to urinary incontinence (UI) in general and stress urinary incontinence (SUI) in particular. SUI is associated with the involuntary leakage of urine on coughing, sneezing, and physical exertion. The severity of SUI increases with age to the extent that it has been termed a hidden epidemic by DeLancey [1]. As a consequence, diagnostic methodologies, collectively called urodynamic testing, evolved to focus on the primary functions of the bladder and urethra as these structures are directly implicated. In cases of SUI, the function of the PF plays a more critical role because of its action on the urethra.

For this reason, it is critical to formalize the evaluation of the function of the PF using a variety of methods ranging from imaging [[2], [3], [4]] to probe development [[5], [6], [7], [8], [9]]. Evidently the technical requirements of PF dynamics instrumentation are more complex and challenging, requiring a contextual approach and the least possible invasive means. In current practice, manual muscle testing per vagina or rectum is the technique used by most clinicians to evaluate the pelvic floor

muscles (PFMs). Unfortunately, due to the location of the PFMs defining their normal function in a noninvasive way is clinically challenging because of the complex 3-D arrangement of muscle groups, as well as the biomechanics of connective tissue and their attachments to the bony pelvis. Moreover there are few diagnostic tools to facilitate the outcome of treatment or objective metrics to document its effectiveness. Unlike urodynamics, PF evaluation has a limited range of dedicated technologies to characterize and localize the extent of dysfunction in a quantitative way. These factors also need to be contrasted by the fact that the physiotherapists contribute, as first responders, in many countries to the treatment of UI using PF training exercises [[10], [11], [12], [13]].

In view of the earlier considerations, in this chapter we will describe methods developed to evaluate PF function in as quantitative a way as possible using our novel technology, parameters, and metrics developed specifically for the purpose. To start with, this chapter is focused toward the noninvasive acquisition of PF function using perineal ultrasound imaging and image processing [14]. Clearly, different biomechanical parameters are generated from these measurements and their utility in the appropriate diagnosis of SUI will await more controlled trials.

Because the fundamental clinical approach in the evaluation of PF function examination is also done using vaginal palpation [14], we shall consider in this chapter a description of a vaginal probe constructed to quantify the biomechanical vaginal closure forces [9]. Data generated using this probe are collected using a protocol of voluntary and reflex activation of the PF of normal subjects and also those with SUI. PF function obtained using our probe is typically invasive because it is inserted into the vagina. The inclusion of data using the vaginal probe can be considered as a complementary method to the digital vaginal examination in that it generates biomechanical outcomes regarding PF function in ways that ultrasound visualization alone does not. As seen in the chapter by Egorov, important biomechanical parameters of tissue constituent properties require direct measurements. Thus, as it will be demonstrated in the following section, while ultrasound can provide information about kinematic parameters such as timing, displacement, velocity acceleration, trajectory, and strain in the PF, it cannot measure the forces that are involved in their generation.

Ultrasound Imaging

Perineal ultrasound imaging has become a method of choice to study the biomechanical characteristics of the female PF [5]. In this chapter, we aim to illustrate some important biomechanical parameters of PF function, which can be helpful in understanding the underlying mechanisms of PF behavior. The dynamic function of PF tissues can be derived from short video segments of ultrasound imaging. To quantitatively derive biomechanical parameters from the image sequences, a coordinate system was established. This coordinate system spans the symphysis, urethra, vagina, and the anorectal junction, all of which are best seen together on a sagittal view. For convenience this coordinate system is overlaid on the sagittal view of the ultrasonogram shown in Fig. 1.

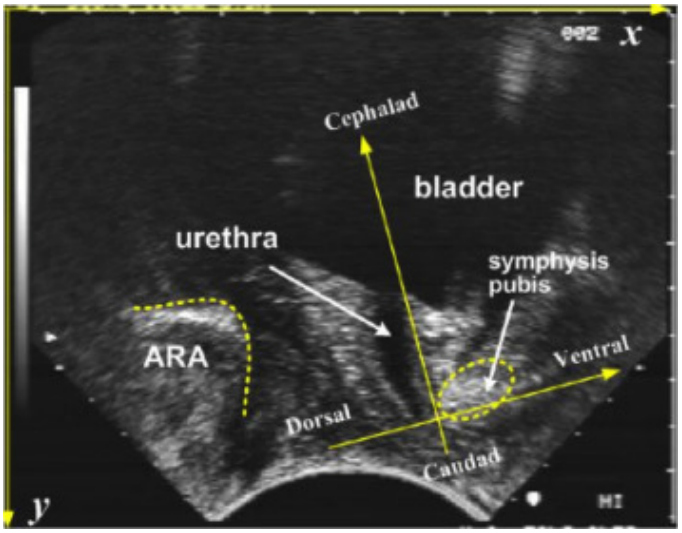

Download: Download full-size image

Figure 1. The orthogonal coordinate system fixed on the symphysis pubis. The two orthogonal components (ventral-dorsal and cephalad-caudad components) of the tissues displacements reflect PF functions of squeezing the urethra and supporting the bladder, respectively.

During rest, strain, and squeeze maneuvers, displacement of the PF tissues can be defined as occurring in one or more directions: anteroposterior and superior-inferior. A ventral (anterior) component moves the tissues closer to the symphysis, whereas a dorsal (posterior) component moves the tissues away from the symphysis pubis. Furthermore, a cephalad (superior) component moves the tissues cranially, and a caudal (inferior) component moves the tissues toward the feet.

The choice of these directions is supported by other studies that suggest that in a functional PFM contraction, the bladder neck has been shown to move in a ventrocephalad direction [15], increasing the closure pressure within the urethra as it is displaced toward the symphysis pubis [16]. During Valsalva, as the intraabdominal pressure increases, the bladder neck moves in a dorsal-caudal direction. Based on these considerations, the orthogonal coordinate system, fixed on the bony landmark, the symphysis pubis, was established (Fig. 1). The two axes of the coordinate system are parallel and vertical to the urethra at rest, respectively. Using this schema, measurements of displacement and time can be made sonographically. From the time and displacement measures, the biomechanically important outcome, velocity of contraction, can be obtained. Acceleration can be derived by numerically differentiating the velocity curve.

Dynamic Ultrasound Image Analysis

As indicated by the ultrasonogram of Fig. 1, the identified anatomical structure is the angle that the rectal ampulla forms with the anal canal as defined as the anorectal angle (ARA). Movement in the ARA during maneuvers can be used to analyze the PFMs function. This is because the levator ani muscles wrap around the anorectal junction, and changes in the levator ani due to contraction and

relaxation can change the position of the anorectal junction. It is well known that displacement of the ARA with respect to the symphysis is closely associated with PFMs activity [17]. As such, tissue displacement over time of the ARA with maneuvers can be defined by their magnitude and direction, with respect to the symphysis.

Such characterization can be accomplished using motion tracking techniques in the cephalocaudad and dorsoventral direction during active voluntary PFMs contractions as well during passive displacement during the Valsalva maneuver. Most importantly, motion tracking can be employed to evaluate the biomechanics of responses during reflex activation such as coughing where the guarding reflex is recruited [18].

Practically speaking, to accurately map the trajectory of the ARA in response to a cough it is necessary to maintain each video frame indexed to the symphysis pubis, which is a stationary, rigid, nondeforming structure. However, the movement of the ultrasound probe in experiments could cause a motion artifact in the image of the symphysis pubis. Therefore, the motion artifact of the symphysis pubis needs to be tracked and subtracted from the motion of the ARA. To accomplish the task of indexing, we developed an adaptive motion tracking algorithm based on a matching template to measure the movement of the symphysis pubis. A similar adaptive matching algorithm is used to track the motion of ARA. However, ARA is a soft tissue structure that deforms, particularly in fast maneuvers like coughing. Therefore, a weight coefficient is introduced to accelerate updating of the template to follow the deformations: to decrease the effect of the size and position of the initial template, manually defined in the first image frame, the tracking procedure is performed four times with different initial templates, and the results are averaged. The relative movement of ARA to the symphysis pubis is then derived by subtracting the motion of symphysis pubis from that of the ARA (Fig. 2).

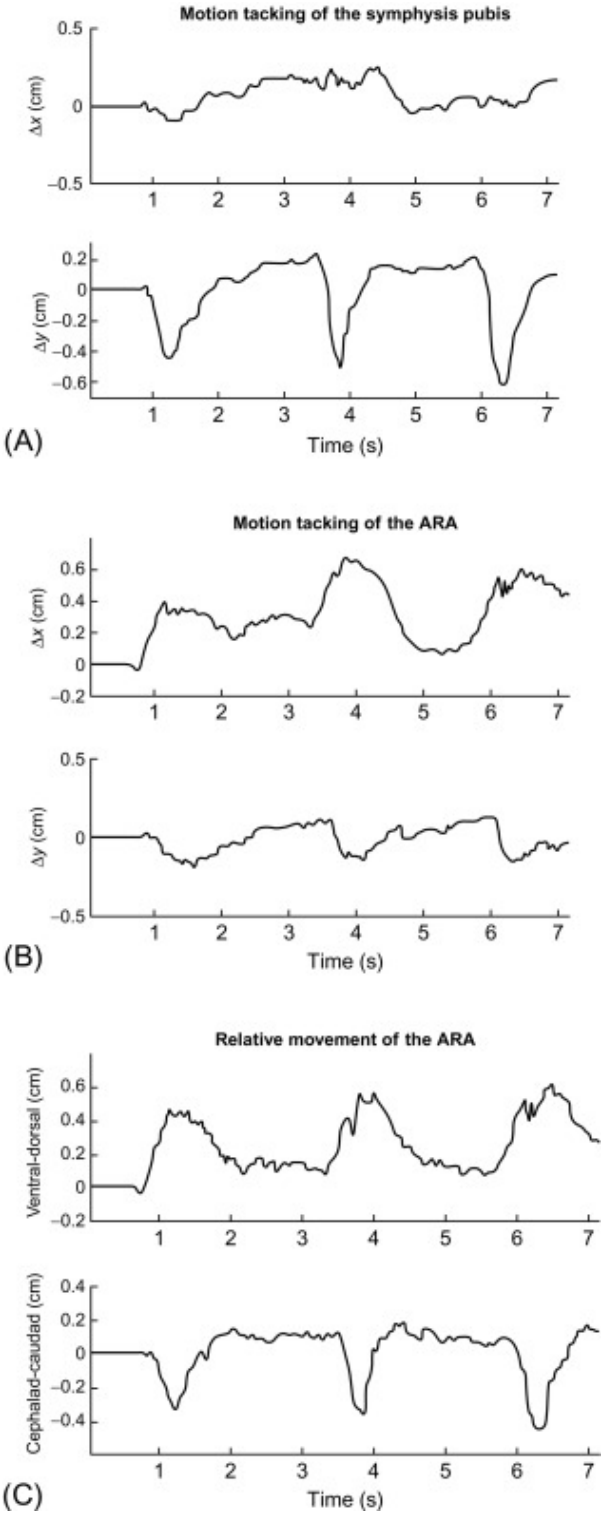

Download: Download full-size image

Figure 2. The motion tracking of (A) the symphysis pubis and (B) the ARA. (C) The ventral-dorsal and cephalad-caudad components of the displacement of the ARA.

Rapid continuous image sequences obtained are recorded and stored for analysis. These video sequences contain dynamic information relating to the integrity of the supporting structures. The resting position of the structures and their displacement at the end of specific and incontinence

producing events (eg, coughing) were measured. However, these methods do not provide information about the path taken by the structures to reach their final destination. Furthermore, due to the speed inherent in such stress events, the observer is unable to be fully informed about the direction of the overall movement at a given moment in time, the velocity at which it occurs, or the acceleration produced. These parameters are important, both in the field of measurement and rehabilitation of the PFMs.

To better understand these kinematic mechanisms, we developed methods to capture and visualize the sequence of dynamic changes the PFMs produced on the urethra, vagina, and rectum. This is made possible by fixing the coordinate system on the symphysis pubis, which is a recognizable stationary landmark across different maneuvers.

Ultrasound movies of normal subjects and SUI patients in coughing were collected and analyzed using those 2-D motion tracking algorithms. Among the parameters evaluated are the trajectory and the maximum displacement vectors of the anorectal junction in coughing (Fig. 3).

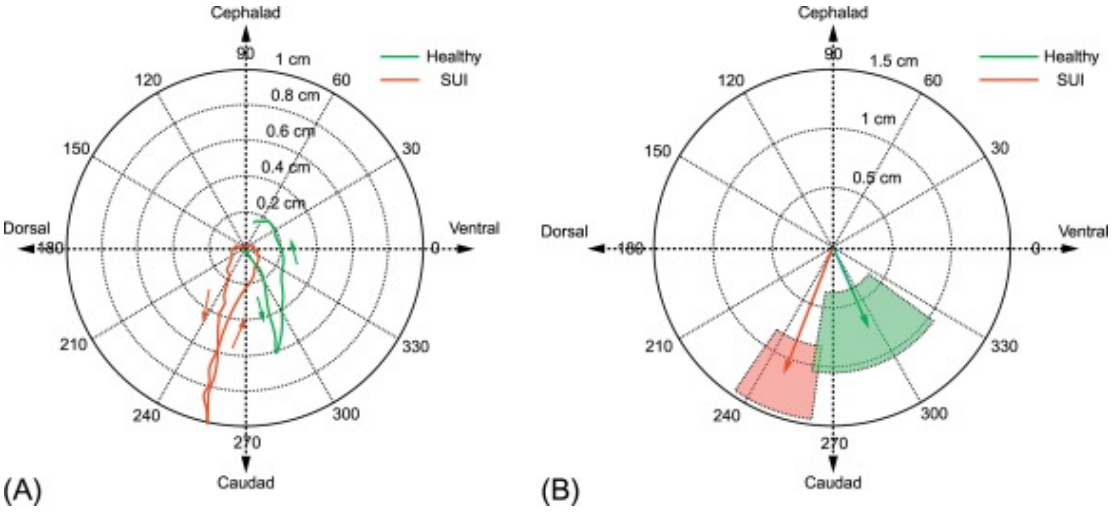

Download: Download full-size image

Figure 3. (A) Trajectory maximum displacement vectors of the anorectal junction in coughing. The normal subjects and SUI patients are shown in *green* and *red,* respectively. (B) The standard deviations are marked by the transparent pies.

The results of the ultrasound experiments show that, when compared to women with SUI, the PFMs of the continent subjects have two mechanisms to prevent urine leakage during stress maneuvers like coughing.

(1) The well-functioning PFMs contractions give the bladder and the posterior edge of the urethra more support in the cephalad direction (green curves in Fig. 4B), when the abdominal pressure increases and pushes the bladder toward the caudad direction in maneuvers like coughing.

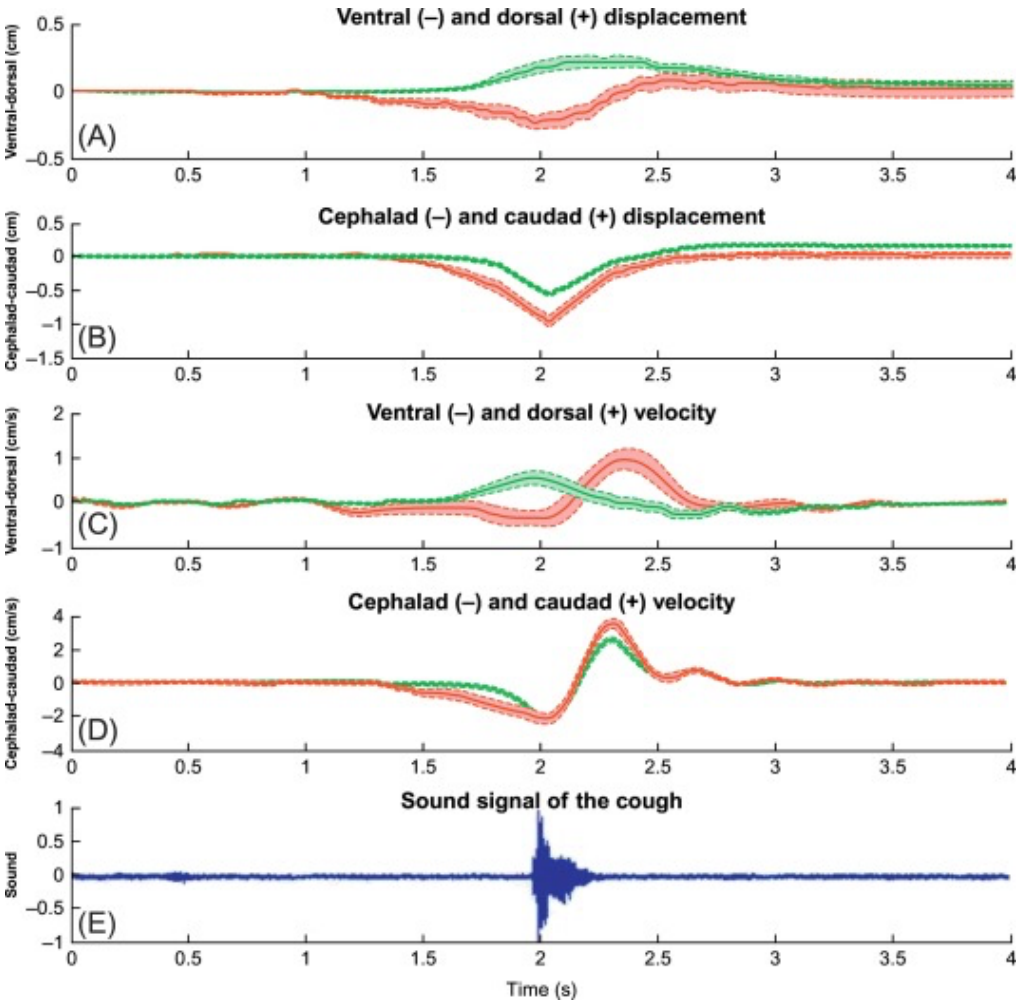

Download: Download full-size image

Figure 4. (A, B) The displacement and (C, D) velocity of the anorectal junction in coughing, and (E) the sound signal. The results of normal subjects and SUI patients are shown in *green* and *red,* respectively.

(2) The well-functioning PFMs contraction pushes the urethra against the symphysis pubis in the dorsal direction and therefore increases the closure pressure in the urethra (green curves in Fig. 4A), when the increased abdominal pressure pushes the urethra toward the ventral direction.

Timing of Pelvic Contractions

The appropriate timing control of the PFMs contraction is as important as, if not more important than, the amplitude of the pressures produced by the PFMs contraction in preventing UI. For this reason, measurements were indexed to the sound recording of the cough, taken by a microphone located on the subject's chest. As shown in Fig. 4A and C, the normal subjects' PFMs contraction pushed the anorectal junction to the dorsal direction (toward the urethra) before the increased

abdominal pressures were able to push the anorectal junction and urethra to the ventral direction. By contrast, the SUI patients' PFMs contractions were behind the increased abdominal pressures in timing. As a result, the anorectal junction and urethra were pushed to the ventral direction at first and then bounded back to the dorsal direction with higher velocity. Those may lead to the decreasing and vibration of the closure pressures in the urethra.

Therefore, an accurate mechanical model to study mechanics of UI should be able to describe not only the closure pressures in the urethra, as most models do, but also the timing, direction, and amplitude of the PFMs contraction produced pressures and how the pressures affect the internal pressures and the movement of the bladder and urethra.

Visualization of the Pathway of Bladder/Urethra and ARA During a Cough

2-D sagittal imaging is useful to document the movement of structures influenced by the PFMs due to voluntary contraction, involuntary reflex events, coughing, or passive forces. Important information, defining the function and effectiveness of the PFMs, was obtained by examining the mechanics of movement of reliably visible organs such as the bladder, urethra, and rectum and define metrics to parameterize and quantify the results. To do so we scanned subjects capturing and storing digitized video sequences of consecutive frames of dynamic ultrasound images. These methods enabled the measurement of timing of movement of pelvic tissues in fast, stressful maneuvers, and facilitated the understanding of the neuromuscular control continence mechanisms. An example of the resulting postprocessed images is given in Figure 5, Figure 6, Figure 7 where transparent color coding based on the segmentation was used to visualize the pathway of timing, amplitude, and direction of movement.

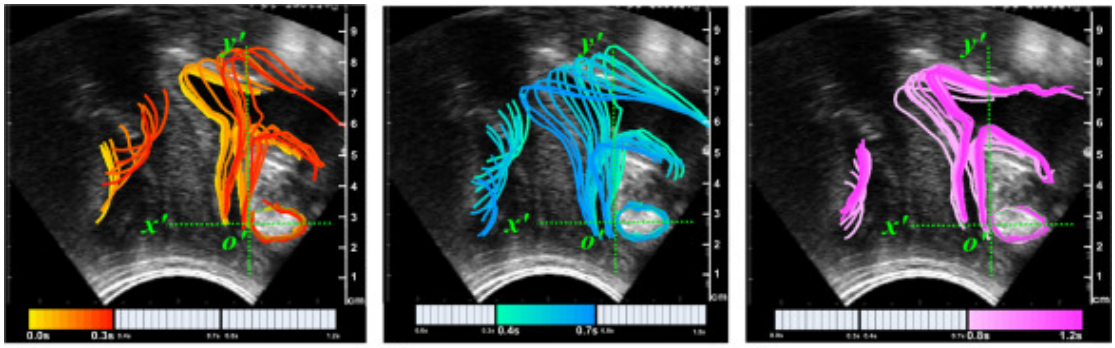

Download: Download full-size image

Figure 5. Frame-by-frame segmentation of outlines of the bladder/urethra, symphysis, and ARA showing the timing and path of displacement. (A) Fast onset; (B) persistence; (C) of the movement of the ARA, bladder, during a single cough.

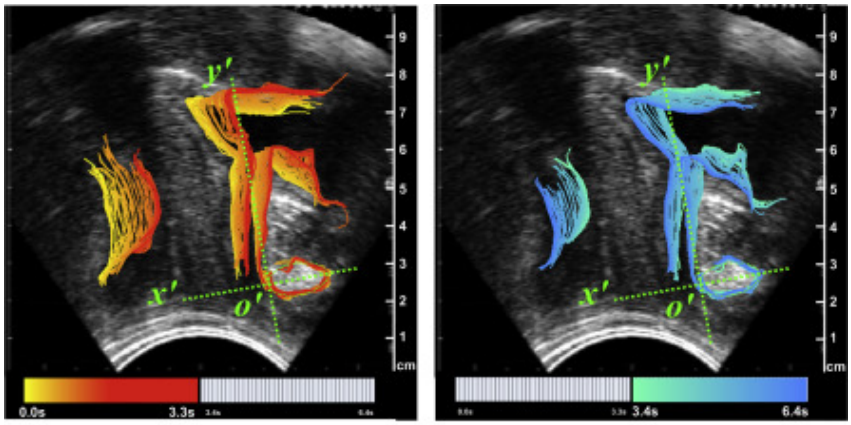

Download: Download full-size image

Figure 6. The timing of the movement due to a voluntary PFMs contraction of 6 s duration. (A) Shows the onset phase of the contraction and (B) release and restoration phase.

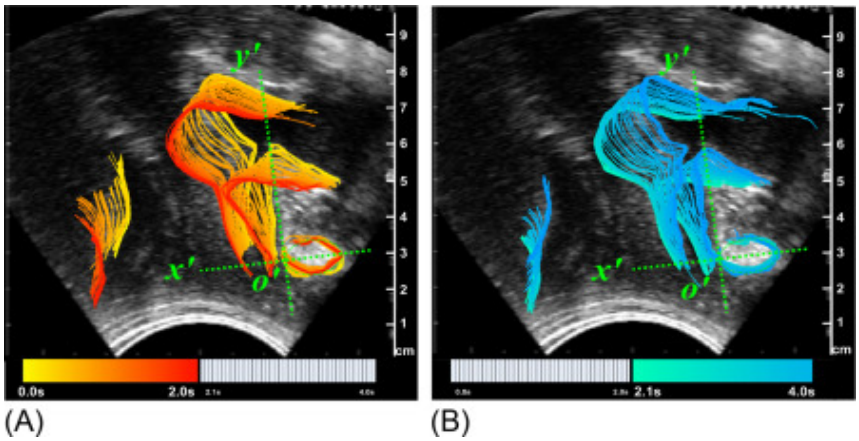

Download: Download full-size image

Figure 7. Time and direction of passive movement during a typical Valsalva of 4 s duration. (A) Represents the onset sequence of a downward movement and (B) return to pre-Valsalva position.

Fig. 5A demonstrates the sequence of displacement of the bladder/urethra as outlined by segmentation, marking the relative movement produced by the reflex contraction of the PFMs during the first 0.3 s. Fig. 5B and C shows the follow-up of PFMs activity. Total recording period is 1.2 s for Fig. 5A–C. Clearly, the human eye cannot retain the detail or quantify the parameters recorded by visual observation during real-time imaging. This visualization using frame-by-frame segmentation of the outlines of bladder/urethra, symphysis, and ARA show the timing and path of displacement where in (a) fast onset of forward movement is shown, (b) the persistance, and (c) of the recovery during a single cough.

Visualization of the Pathway of Bladder/Urethra and ARA During Voluntary PFMs

Contraction

Unlike the pattern of fast displacements produced by the reflex action generated by a cough (Fig. 5), voluntary PFMs contraction has a slower time course. As an example, Fig. 6A illustrates the displacement sequence and timing during a typical voluntary PFMs contraction. As the PFMs contraction starts (Fig. 6A), structures move in a ventral-cephalad direction, forward and up and relaxation (Fig. 6B) return to the original resting position occurs. However, during a cough (Fig. 5), the pattern of response of PFMs muscles differ, suggesting the variance of voluntary to reflex contractions.

Comparison between the pattern shown in Fig. 5, showing the reflex response of the PFMs muscles, and Fig. 6, the voluntary activation of PFMs contractions, provides evidence that while the direction is the same, the time course differs significantly.

Visualization of the Pathways of Bladder/Urethra and ARA During Valsalva

While Fig. 6 shows the timing and displacement caused by voluntary PFMs contraction the response during the passive compression produced by voluntarily straining or Valsalva, structures move from their resting position in a dorsal-caudal direction, down and back before returning to their resting position. Clearly, the response of the active contraction produced by PFMs contraction compared to the passive displacement produced by Valsalva also differ in the ways that may produce some insight into the mechanisms involved in their recruitment.

Clearly, as Fig. 7 shows, the functional PFMs in continent females appear to be highly regulated. These observations provide convincing evidence to support the hypothesis that structures prior to and during a cough appear to be acting like a feedback control system, to resist or limit the dorsal-caudal movement that occurs as during a cough. This hypothesis is supported by comparing both the overall direction and magnitude of displacement. On the basis of these imaging observations, evidence suggests that the function of the PFMs can be quantified and mechanistic insight can be found by appropriate analysis. However, there are important limitations using 2-D ultrasound so that it is not possible to incorporate the contribution of all muscle groups. In that sense the potential use of 3-/4-D imaging needs to be explored using similar analytics so that visualizations are not done only in a single plane.

Strain Analysis of 2-D Dynamic Ultrasound Images

In analogy to the use of ultrasound to evaluate cardiac function, measurements of PFMs strain, a dimensionless index reflecting the deformation produced by contraction can be applied [19]. Details of the methodology used for the PF can be found in Ref. [20] where the generated strain was calculated from the displacement due to the dorsal-ventral and cardinal-caudal displacements of the selected landmarks. From these displacement measurements, shown diagrammatically by Fig. 8 where the displacement generated was simplified to a straight line, strain was calculated as follows:

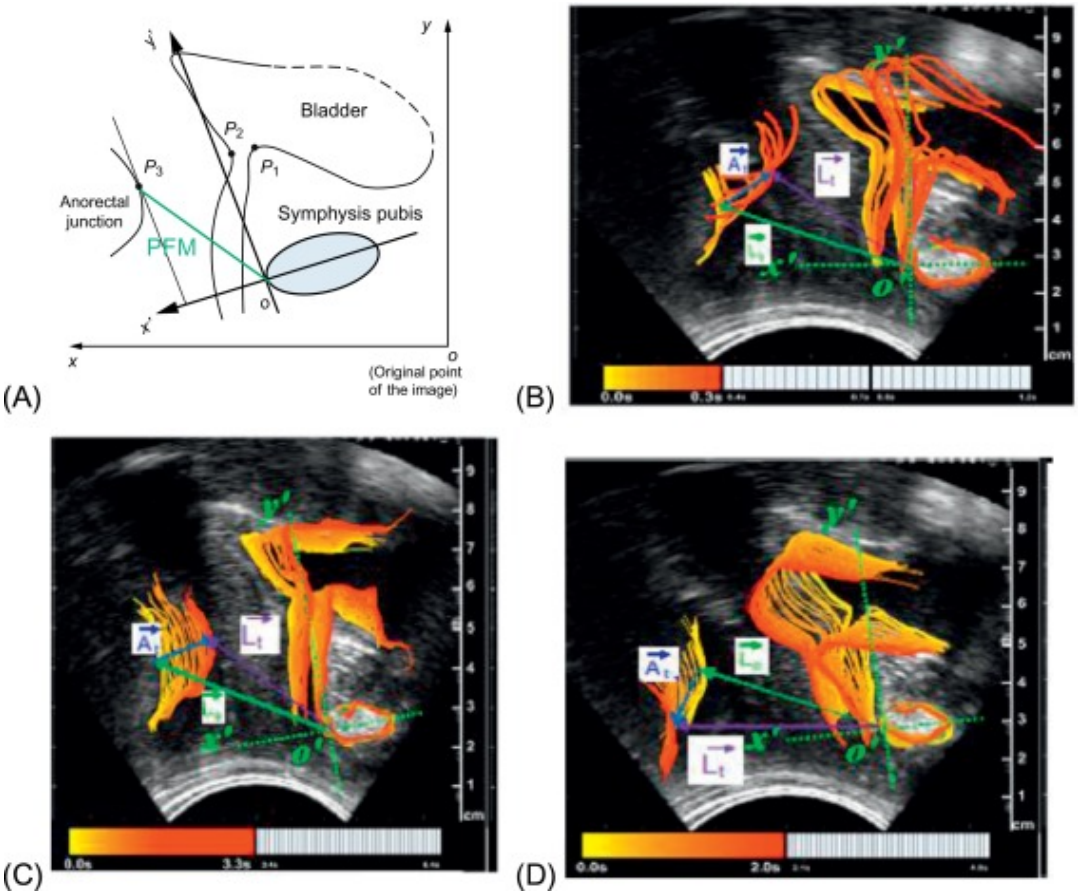

Download: Download full-size image

Figure 8. Diagrammatic presentation of measurements (A) to calculate strain indexed to ultrasound images identifying the outline of bladder/urethra and ARA trajectory [20]. (B) Cough response. (C) Voluntary Contraction. (D) Valsalva.

The strain ε at time t is defined as

$$\varepsilon_t = \frac{\|\dot{L}_t\| - \|\dot{L}_0\|}{\left\|\vec{\dot{L}}_0\right\|}, \tag{1}$$

where $\|\dot{L}_0\|$ is the initial length of the PFM at rest and is measured from the ultrasound images; $\|\dot{L}_t\|$ is the length of the muscle at time t and is calculated from the equation.

$$\left\|\vec{\dot{L}}_t\right\| = \sqrt{\left(\vec{\dot{l}}_{t,x}\right)^2 + \left(\vec{\dot{l}}_{t,y}\right)}. \tag{2}$$

$\dot{l}_{t,x}$ is the vector representing the dorsal-ventral component at time t and is measured by the equation

$$\dot{l}_{t,x} = \Delta\dot{x}_t + \dot{l}_{0,x}. \tag{3}$$

Likewise, $\dot{l}_{t,y}$ is the vector representing cardinal-caudal component at time t and is defined by the

equation

$$\dot{l}_{t,y} = \Delta\dot{y}_t + \dot{l}_{0,y}, \tag{4}$$

where $\dot{l}_{0,x}$ and $\dot{l}_{0,y}$ are the dorsal-ventral and cardinal-caudal vector components at rest (t = 0), respectively. $\Delta\dot{x}_t$ and $\Delta\dot{y}_t$ are the dorsal-ventral and cardinal-caudal displacements, respectively, at time t, which can be measured from the previous displacement measurements. $\dot{A}_t$ represents the vector ($\langle\Delta\dot{x}_t, \Delta\dot{y}_t\rangle$).

To carry out the vector addition, it is necessary to retrieve the $\Delta\dot{x}_t$ and $\Delta\dot{y}_t$ values from the images and add the two vectors (dorsal-ventral and cardinal-caudal components) together; that is, the obtained displacement values of the two components need to be matched to the same time measurement. After the time measurements are matched, the mean of those values will be calculated, and an array made for the average time measurements. Displacement measurements in the dorsal-ventral and cardinal-caudal directions corresponding to those average time values will be added from the data files to that array. Vectors $\dot{l}_{0,x}$ and $\dot{l}_{0,y}$, shown in Fig. 5, will be added to the corresponding displacement measurements according to Eqs. (3), (4) and strain calculated according to Eq. (2) at each of the time values. A strain versus time graph will be plotted for each of the four maneuvers in the supine position and in the standing position for the case of cough in both asymptomatic and UI patients. Subsequently, the maximum strain of the PFMs for both groups is obtained and statistical comparisons between the two groups are carried out.

Strain rate (SR) measurements: Using these displacement measurements along with the velocity measurements, the *SR* of PFMs for asymptomatic and incontinent women during a cough was calculated.

SR can be measured using the following equation:

$$\frac{dL}{L} \approx \frac{v(r+\Delta r)-v(r)}{\Delta r}dt = SR\,dt, \tag{5}$$

where here r represents the position of the point on the ARA, thus $\Delta r = \left|\left|\dot{L}_t\right|\right|$, which is defined by Eq. (2).

Also,

$$v(r+\Delta r)-v(r) = \Delta v = \sqrt{(\Delta v_x)^2 + (\Delta v_y)^2}. \tag{6}$$

SR is related to strain by the equation

$$\varepsilon = \exp\left(\int_{t_0}^{t} SR\,dt\right) - 1, \tag{7}$$

and that is because *SR* is defined as the time derivative of natural strain $\left(\ln\frac{L}{L_0}\right)$.

From Eq. (5) the *SR* will be calculated using the same algorithm and the matching algorithm as described earlier for strain measurement, with the addition that now the time measurement needs to be matched for both velocity and displacement in the dorsal-ventral and cardinal-caudal direction. Thus, the mean time value is calculated by averaging the four matched values, and the similar method described in the strain measurement using Microsoft Excel is used to apply Eq. (6) to all the collected data points. *SR* versus time is graphed for the two groups and the maximum *SR* is calculated and compared for significant differences.

Elastic Properties

The in vivo biomechanical analysis that is facilitated by the ultrasound imaging as described earlier, where the length and displacement are measured from the images, incorporates the elastic properties of the vaginal and urethral tissues. The response measured inevitably involves the complex interactions between mechanical forces, and neurological, muscular, and connective tissue factors [21]. Currently there is incomplete understanding of how tissue composition contributes to its function or its biomechanical properties. Due to methodological limitations it is challenging to perform biomechanical and biochemical testing on the same tissue. Also, most biomechanical data are on tissue from affected individuals while little is known about asymptomatic, unaffected tissue. Safety considerations limit our ability to obtain large tissue samples from asymptomatic controls. Most evaluation of the biomechanical properties of vaginal tissue in patients with clinical problems is done using a variation of the uniaxial loading technique to test tissue biomechanics. This technique is commonly used to characterize the elastic, viscous, and plastic properties of vaginal tissue. This methodology is limited, in that it only provides 1-D force displacement characteristics requiring large pieces to obtain a homogeneous stress state.

A novel evaluation of tissue properties was done where an evaluation of human vaginal wall stiffness was correlated with measurements to collagen expression in women with and without pelvic organ prolapse (POP) [21]. The results of these studies are demonstrated in Fig. 11, which shows the difference in the 2-D distribution of stiffness between prolapse patients and controls.

A biomechanical comparison of the elasticity of vaginal wall tissues in terms of the tangent modulus of elasticity can then be thus compared using vaginal wall tissue mapping (Fig. 9A). Vertical axis and color maps show stiffness in kilopascal. Red areas represent greater stiffness. Blue areas represent less stiff material. A stiffness distribution histogram shows that tissue from a patient with prolapse was on average stiffer than control tissue.

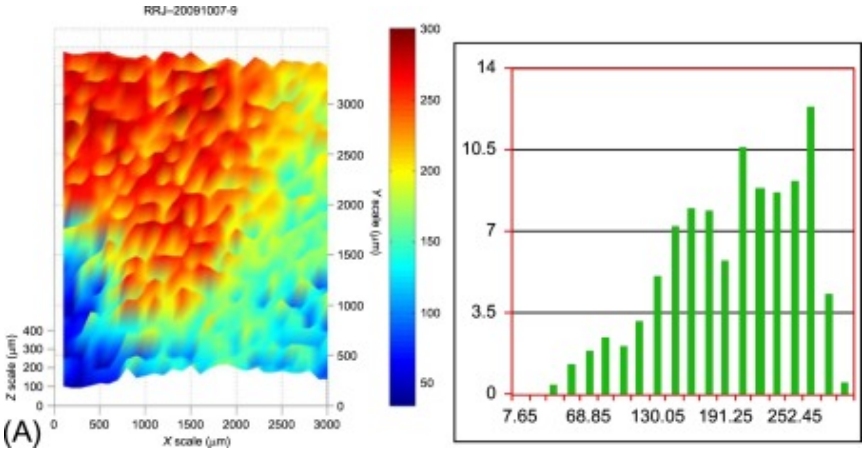

Download: Download full-size image

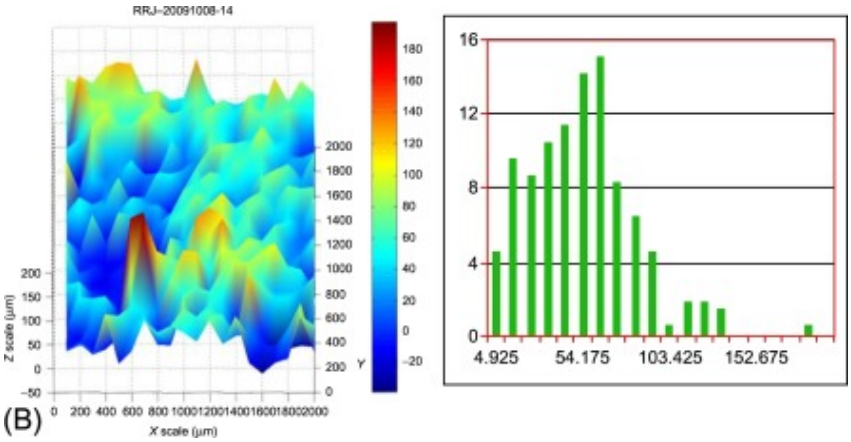

Download: Download full-size image

Figure 9. (A) Distribution of stiffness in a 78-year-old woman with prolapse. (B) Distribution of stiffness of an 80-year-old continent woman.

In this study, we evaluated vaginal tissue biomechanics in women with and without POP and confirmed that collagen type I and III composition is associated with measureable tissue biomechanics. We observed that the vaginal wall was stiffer in cases than in controls. Results are consistent with data from a study using a proof of concept prototype of the vaginal tactile imager of Egorov et al. [8] and with data obtained by traditional uniaxial tension tests. Overall the traditional uniaxial tension studies indicate that prolapse confers less elasticity and greater stiffness with low forces at failure. Our data are consistent with this and indicate that the use of a piezoelectric scanning probe is a reliable way to measure tissue biomechanics without the need for large tissue samples. From the biomechanics point of view, collagen type I is nonelastic and confers great resistance to tensile forces while collagen III has elastic properties and prevails in more flexible tissue [21,22].

Vaginal Probe

While aspects of PF function can be evaluated using the imaging techniques afforded by ultrasound above with the possibility of identifying mechanism of function and anatomical defects, in current clinical practice, digital vaginal examinations are necessarily performed. Such testing provides qualitative information about pathology but invariably do not generate quantitative measures to characterize the ability of the subject to function, as such conservative approaches to strengthen PF function remain subjective and operator dependant [[10], [11], [12], [13], [14]]. There is therefore a need to document the magnitude and direction of the biomechanical forces produced around the length of the vagina as well as active forces during voluntary contraction or the reflexes during coughing. Because the accuracy of the digital vaginal palpation is highly dependent on the experiences of the examiner and the ability to document it, it has become essential to design and build devices that can accomplish a more biomechanically accurate measure. A number of such devices have been evaluated and the results reported in the literature [[6], [7], [8], [9]], each of which has specific characteristics and usefulness to its creator. Commercial devices are beginning to enter the marketplace. In this chapter, we will present the principles of our sensor system, shown in Fig. 10, designed to measure the mechanical characteristics of the vaginal wall and the amplitude of the pressure produced by the PFMs. The system is made of a probe with four force and displacement sensors and a six-degrees-of-freedom measuring device that can track the position (x, y, z) and orientation (azimuth, elevation, and roll angles) of the probe. The probe is made of an applicator with retractable low inertia cantilevered force and displacement transducers in four directions (anterior, posterior, left, and right). For patient protection, the probe is inserted in the vagina using a female condom placed over the sensors. Once the probe is in place, a diameter adjustor is gradually released to allow opening from its retracted position so that the transducers make contact with the vaginal wall. The vaginal pressure of 25 normal subjects and 10 patients with SUI are measured in supine by using this sensor system.

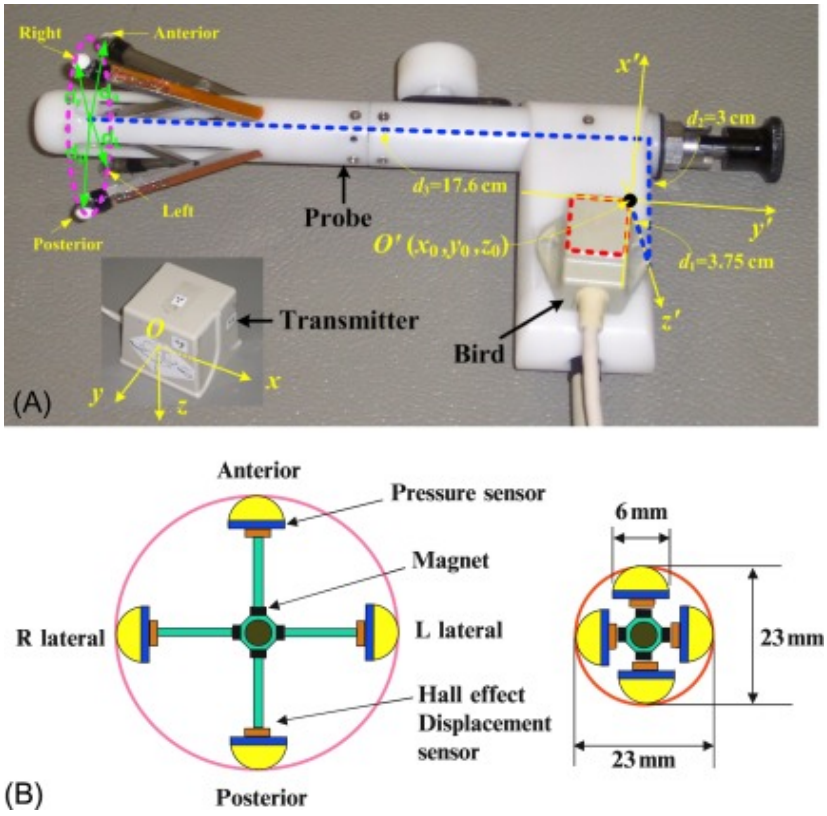

Download: Download full-size image

Figure 10. (A) The picture of the sensor system and (B) the cross section of the probe.

The results show that the normal subjects have significantly higher mean contact pressure of the PFMs side of the vagina both at rest (healthy: 1.67 ± 0.13 N/cm^2, SUI: 1.15 ± 0.18 N/cm^2, p = 0.048) and with 50% PFMs contraction (healthy: 2.05 ± 0.13 N/cm^2, SUI: 1.35 ± 0.20 N/cm^2, p = 0.009). Using this probe, a profile of contact pressures of the normal subjects and the SUI patients is illustrated by Fig. 11, showing the distribution of pressures is higher in the anterior aspect of the vagina compared to the posterior. Activation of PF contraction at 50% maximum shows the relative increase.

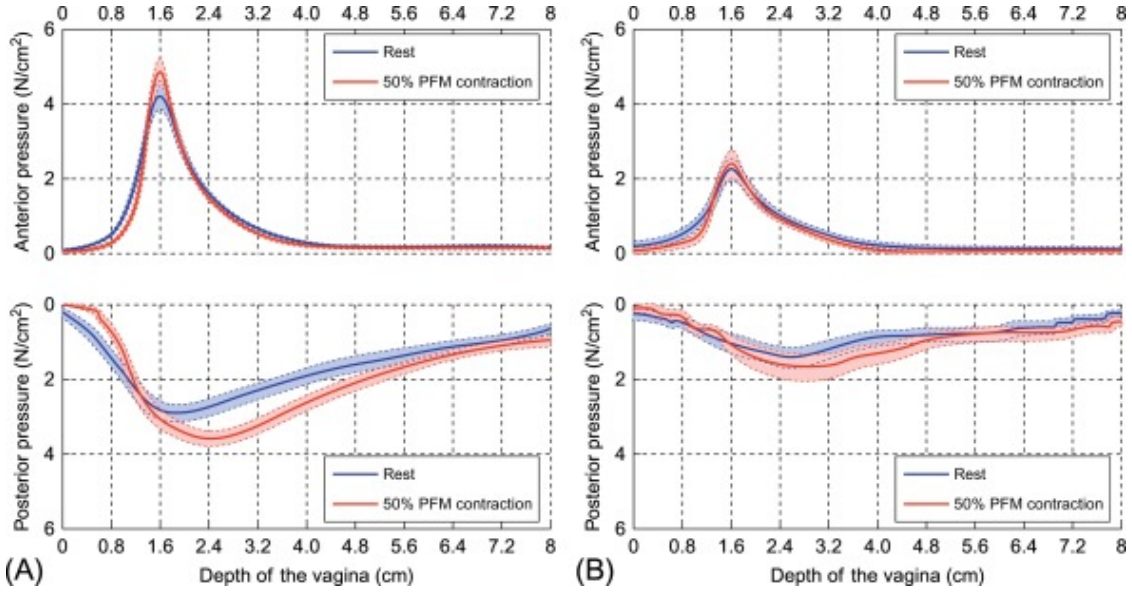

Download: Download full-size image

Figure 11. Vaginal contact pressure profile of (A) controls and (B) SUI subjects. Horizontal axis is depth into the vagina and vertical axis is the contact pressure. Mechanically, the probe shown in Fig. 1 contains four sensors and interpolation of the contact forces measured can be used to demonstrate the full 360 degrees distribution of closure.

In recent times, a number of vaginal probes using different construction have been developed, some of which evaluate the tissue elastic properties instead of contact pressure [8]. It is important to indicate that probing the vaginal wall asymmetric values of closure are obtained. Fig. 12 graphically shows that maximal closure is measured in the anterior aspect of the vaginal wall.

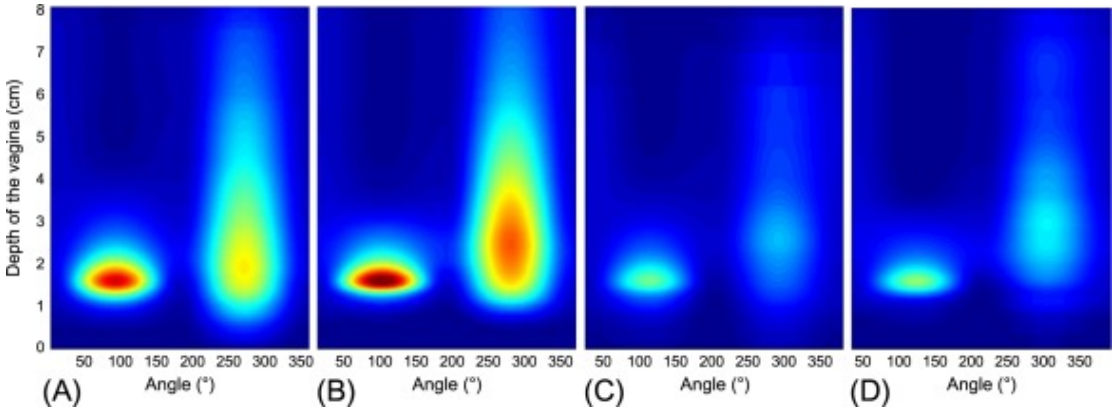

Download: Download full-size image

Figure 12. Distribution of vaginal closure over 360 degrees. (A) Shows closure at rest and (B) following PF contraction. Similarly (C) and (D) but in subjects with SUI.

As shown in Fig. 12, maximal closure is located 1.5 cm from the introitus in its anterior subject for all subjects and lower at the posterior aspect. Incontinent women possess numerically lower closure

with a region of lower stiffness as measured by Egorov in a different chapter of this book.

Clearly with this and similar technology such as the instrumented speculum, incontinent women demonstrated lower values in passive force, endurance, and speed of contraction than continent women [6,7]. Given that PFMs strengthening exercises diminish the symptoms of SUI [10,11,23], it is therefore important to resolve whether the mechanisms involved in therapeutic changes to help identify the specific critical muscle components involved. It is unknown whether the PF exercises mimics the normal physiological behavior of the PFMs or is a compensation strategy. Nonetheless a program of awareness is indeed the most efficient method of implementing rehabilitation. To do so it is appropriate to best understand the many facets of function and to impart this information to the patient.

Summary of Ultrasound Imaging Parameters

Perineal ultrasound imaging provides a convenient and noninvasive way to evaluate PF function documenting the biomechanical metrics involved. It was shown that timing of reflex PF contractions is critical in maintaining urinary continence. Pelvic organ displacement from a resting state as a result of Valsalva indicates the state of the ligaments and the stiffness of the supporting structures as the body of the uterus, the bladder, and the rectal portion of the PFMs evidenced the highest displacement during Valsalva. The magnitude of the displacement of the bladder during voluntary PF contraction can be considered an indicator of muscle strength. It was shown that the tissue elasticity of the vaginal wall plays a significant role in the overall mechanisms involved in the maintenance of continence. Biomechanically functional parameters were identified using a number of analytical approaches.

In conclusion we have demonstrated that in focusing on the biomechanics of PF function using noninvasive ultrasound, the following metrics for each testing protocol have been identified: displacement, velocity, acceleration, trajectory, timing, and strain. However, these values depend on other parameters such as the elastic properties of the tissues and the strength of the contraction. Invasive methods such as a vaginal probe are necessary to document the strength of PF contractility. Such probing devices can be used to assess physiotherapy interventions or other treatment regiments.

References

[1] J.O. DeLancey
The hidden epidemic of pelvic floor dysfunction: achievable goals for improved prevention and treatment
Am. J. Obstet. Gynecol., 192 (5) (2005), pp. 1488-1495

View PDF View article View in Scopus ↗ Google Scholar ↗

[2] S.H. Yang, W.C. Huang, S.Y. Yang, E. Yang, J.M. Yang
Validation of new ultrasound parameters for quantifying pelvic floor muscle contraction
Ultrasound Obstet. Gynecol., 144 (Suppl. 1) (2009), pp. S159-S165
Review
View in Scopus ↗ Google Scholar ↗

[3] C.E. Constantinou
Dynamics of female pelvic floor function using urodynamics, ultrasound and magnetic resonance imaging (MRI)
Eur. J. Obstet. Gynecol. Reprod. Biol., 144 (Suppl. 1) (2009), pp. S159-S165, 10.1016/j.ejogrb.2009.02.021 ↗
Review
View PDF View article View in Scopus ↗ Google Scholar ↗

[4] R.C. Lovegrove Jones, Q. Peng, M. Stokes, V.F. Humphrey, C. Payne, C.E. Constantinou
Mechanisms of pelvic floor muscle function and the effect on the urethra during a cough
Eur. Urol., 57 (6) (2010), pp. 1101-1110, 10.1016/j.eururo.2009.06.011 ↗
PMID:
19560261 ↗
View PDF View article View in Scopus ↗ Google Scholar ↗

[5] H.P. Dietz, M. Erdmann, K.L. Shek
Reflex contraction of the levator ani in women symptomatic for pelvic floor disorders
Ultrasound Obstet. Gynecol., 40 (2) (2012), pp. 215-218, 10.1002/uog.11087 ↗
PMID:
22223551 ↗
View in Scopus ↗ Google Scholar ↗

[6] J.M. Miller, J.A. Ashton-Miller, D. Perruchini, J.O. DeLancey
Test-retest reliability of an instrumented speculum for measuring vaginal closure force
Neurourol. Urodyn., 26 (6) (2007), pp. 858-863
Crossref ↗ View in Scopus ↗ Google Scholar ↗

[7] M. Morin, D. Gravel, D. Bourbonnais, C. Dumoulin, S. Ouellet
Reliability of dynamometric passive properties of the pelvic floor muscles in postmenopausal women with stress urinary incontinence

Neurourol. Urodyn., 27 (8) (2008), pp. 819-825

Crossref ↗ View in Scopus ↗ Google Scholar ↗

[8] V. Egorov, H. van Raalte, A.P. Sarvazyan

Vaginal tactile imaging

IEEE Trans. Biomed. Eng., 57 (7) (2010), pp. 1736-1744, 10.1109/TBME.2010.2045757 ↗

PMID:

20483695 ↗

View in Scopus ↗ Google Scholar ↗

[9] C.E. Constantinou, S. Omata

Direction sensitive sensor probe for the evaluation of voluntary and reflex pelvic floor contractions

Neurourol. Urodyn., 26 (3) (2007), pp. 386-391

PMID:

17301962 ↗

Crossref ↗ View in Scopus ↗ Google Scholar ↗

[10] K. Bø, G. Hilde, J. Stær-Jensen, F. Siafarikas, M.K. Tennfjord, M.E. Engh

Postpartum pelvic floor muscle training and pelvic organ prolapse — a randomized trial of primiparous women

Am. J. Obstet. Gynecol., 212 (1) (2015), pp. 38.e1-38.e7, 10.1016/j.ajog.2014.06.049 ↗

PMID:

24983687 ↗

View PDF View article Google Scholar ↗

[11] K. Bø, G. Hilde, M.K. Tennfjord, J. Stær-Jensen, F. Siafarikas, M.E. Engh

Pelvic floor muscle variables and levator hiatus dimensions: a 3/4D transperineal ultrasound cross-sectional study on 300 nulliparous pregnant women

Int. Urogynecol. J., 25 (10) (2014), pp. 1357-1361, 10.1007/s00192-014-2408-8 ↗

PMID:

24828605 ↗

View in Scopus ↗ Google Scholar ↗

[12] F. Siafarikas, J. Stær-Jensen, G. Hilde, K. Bø, M. Ellström Engh

Levator hiatus dimensions in late pregnancy and the process of labor: a 3- and 4-dimensional transperineal ultrasound study

Am. J. Obstet. Gynecol., 210 (5) (2014), pp. 484.e1-484.e7, 10.1016/j.ajog.2014.02.021 ↗

PMID:

24569040 ↗

View PDF View article Google Scholar ↗

[13] J.A. Thompson, P.B. O'Sullivan, N.K. Briffa, P. Neumann
Differences in muscle activation patterns during pelvic floor muscle contraction and Valsalva maneuver
Neurourol. Urodyn., 25 (2) (2006), pp. 148-155
PMID:
16302270 ↗
Crossref ↗ View in Scopus ↗ Google Scholar ↗

[14] I. Volløyhaug, S. Mørkved, Ø. Salvesen, K.Å. Salvesen
Assessment of pelvic floor muscle contraction with palpation, perineometry and transperineal ultrasound: a cross-sectional study
Ultrasound Obstet. Gynecol. (2015), 10.1002/uog.15731 ↗
Google Scholar ↗

[15] J.M. Miller, J.A. Ashton-Miller, J.O. DeLancey
A pelvic muscle precontraction can reduce cough-related urine loss in selected women with mild SUI
J. Am. Geriatr. Soc., 46 (7) (1998), pp. 870-874
PMID:
9670874 ↗
Crossref ↗ View in Scopus ↗ Google Scholar ↗

[16] D. Howard, J.M. Miller, J.O. Delancey, J.A. Ashton-Miller
Differential effects of cough, valsalva, and continence status on vesical neck movement
Obstet. Gynecol., 95 (4) (2000), pp. 535-540
PMID:
10725485 ↗
View PDF View article View in Scopus ↗ Google Scholar ↗

[17] C.E. Constantinou, D.E. Govan
Spatial distribution and timing of transmitted and reflexly generated urethral pressures in healthy women
J. Urol., 127 (5) (1982), pp. 964-969
PMID:
7201031 ↗
View PDF View article Crossref ↗ View in Scopus ↗ Google Scholar ↗

[18] G.C. Nesbitt, S. Mankad
Strain and strain rate imaging in cardiomyopathy
Echocardiography, 26 (2009), pp. 337-344

Crossref ↗ View in Scopus ↗ Google Scholar ↗

[19] S. Rahmanian, R. Jones, Q. Peng, C.E. Constantinou
Visualization of biomechanical properties of female pelvic floor function using video motion tracking of ultrasound imaging
Stud. Health Technol. Inform., 132 (2008), pp. 390-395
PMID:
18391328 ↗
View in Scopus ↗ Google Scholar ↗

[20] L. Zhou, J.H. Lee, Y. Wen, C. Constantinou, M. Yoshinobu, S. Omata, B. Chen
Biomechanical properties and associated collagen composition in vaginal tissue of women with pelvic organ prolapse
J. Urol., 188 (3) (2012), pp. 875-880, 10.1016/j.juro.2012.05.017 ↗
PMID:
22819408 ↗
View PDF View article View in Scopus ↗ Google Scholar ↗

[21] P. Chantereau, M. Brieu, M. Kammal, J. Farthmann, B. Gabriel, M. Cosson
Mechanical properties of pelvic soft tissue of young women and impact of aging
Int. Urogynecol. J., 25 (11) (2014), pp. 1547-1553, 10.1007/s00192-014-2439-1 ↗
PMID:
25007897 ↗
View in Scopus ↗ Google Scholar ↗

[22] P.A. Norton
Pelvic floor disorders: the role of fascia and ligaments
Clin. Obstet. Gynecol., 36 (4) (1993), pp. 926-938
PMID:
8293593 ↗
Review
Crossref ↗ View in Scopus ↗ Google Scholar ↗

Cited by (1)

Position and orientation of vaginal pessaries in situ on magnetic resonance imaging ↗
2022, International Urogynecology Journal

View Abstract